Quantum Corrections to Symmetron Fifth Forces

2508.16726

Michael Udemba

University of Manchester

December 18, 2025

Why Study Scalar Fields?

Why Study Scalar Fields?

Scalar fields turn up frequently in the proposed solutions to problems in the Standard Model of Particle Physics and ΛCDM.

Why Study Scalar Fields?

Scalar fields turn up frequently in the proposed solutions to problems in the Standard Model of Particle Physics and ΛCDM.

- Hierarchy problem
- Quantum gravity
- Strong CP problem

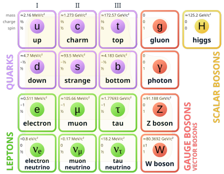

Why Study Scalar Fields?

Scalar fields turn up frequently in the proposed solutions to problems in the Standard Model of Particle Physics and ΛCDM.

- Hierarchy problem
- Quantum gravity
- Strong CP problem

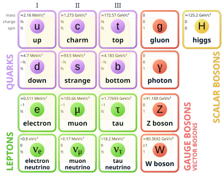

- Inflation
- Dark energy
- Dark matter

Scalar-Tensor Theory

Scalar-Tensor Theory

Roughly speaking, couple a scalar field ϕ to the metric tensor.

Scalar-Tensor Theory

Roughly speaking, couple a scalar field ϕ to the metric tensor. More precisely...

$$S = \int \mathrm{d}^4x \sqrt{-g} R + \int \mathrm{d}^4x \sqrt{-\tilde{g}} \mathscr{L}_{\text{matter}} \left(\tilde{g}_{\mu\nu}\right) + \int \mathrm{d}^4x \sqrt{-g} \left(-\frac{1}{2} \partial_\mu \phi \partial^\mu \phi - V(\phi)\right) \tag{1}$$

Scalar-Tensor Theory

Roughly speaking, couple a scalar field ϕ to the metric tensor. More precisely...

$$S = \int \mathrm{d}^4x \sqrt{-g}R + \int \mathrm{d}^4x \sqrt{-\tilde{g}}\mathscr{L}_{\text{matter}}\left(\tilde{g}_{\mu\nu}\right) + \int \mathrm{d}^4x \sqrt{-g}\left(-\frac{1}{2}\partial_\mu\phi\,\partial^\mu\phi - V(\phi)\right) \tag{1}$$

Physically equivalent conformal frames $g_{\mu\nu}$ and $\tilde{g}_{\mu\nu} = A(\phi)^2 g_{\mu\nu}$.

Scalar-Tensor Theory

Roughly speaking, couple a scalar field ϕ to the metric tensor. More precisely...

$$S = \int \mathrm{d}^4x \sqrt{-g}R + \int \mathrm{d}^4x \sqrt{-\tilde{g}}\mathscr{L}_{\mathrm{matter}}\left(\tilde{g}_{\mu\nu}\right) + \int \mathrm{d}^4x \sqrt{-g}\left(-\frac{1}{2}\partial_\mu\phi\,\partial^\mu\phi - V(\phi)\right) \tag{1}$$

Physically equivalent conformal frames $g_{\mu\nu}$ and $\tilde{g}_{\mu\nu} = A(\phi)^2 g_{\mu\nu}$.

Observational effects: Contribution to vacuum energy (dark energy or inflation), fifth forces (dark matter).

Screened Modified Gravity

Screened Modified Gravity

Question: If there is a fifth force, why haven't we seen it yet?

Screened Modified Gravity

Question: If there is a fifth force, why haven't we seen it yet?

Answer: Screening – some mechanism which hides fifth forces from local tests.

Screened Modified Gravity

Question: If there is a fifth force, why haven't we seen it yet?

Answer: Screening – some mechanism which hides fifth forces from local tests.

Tends to require nonlinearities in the field's equation of motion.

Screened Modified Gravity

Question: If there is a fifth force, why haven't we seen it yet?

Answer: Screening – some mechanism which hides fifth forces from local tests.

Tends to require nonlinearities in the field's equation of motion.

Example: The chamelon model. The mass m of the scalar is proportional to ambient density of matter. The range of the fifth force goes like m^{-1}.

The Symmetron Model

The Symmetron Model

$$A(\phi) = 1 + \frac{\phi^2}{2M^2}$$

$$V(\phi) = -\frac{1}{2}\mu^2\phi^2 + \frac{1}{4}\lambda\phi^4$$

$$V_{\mathrm{eff}}(\phi) = \frac{1}{2}\left(\frac{\rho}{M^2} - \mu^2\right)\phi^2 + \frac{1}{4}\lambda\phi^4$$

$\rho \rightarrow$ background matter density
$M \rightarrow$ matter coupling
$\mu \rightarrow$ mass term
$\lambda \rightarrow$ dimensionless self-coupling

The Symmetron Model

$$A(\phi) = 1 + \frac{\phi^2}{2M^2}$$

$$V(\phi) = -\frac{1}{2}\mu^2\phi^2 + \frac{1}{4}\lambda\phi^4$$

$$V_{\text{eff}}(\phi) = \frac{1}{2}\left(\frac{\rho}{M^2} - \mu^2\right)\phi^2 + \frac{1}{4}\lambda\phi^4$$

$\rho \longrightarrow$ background matter density
$M \longrightarrow$ matter coupling
$\mu \longrightarrow$ mass term
$\lambda \longrightarrow$ dimensionless self-coupling

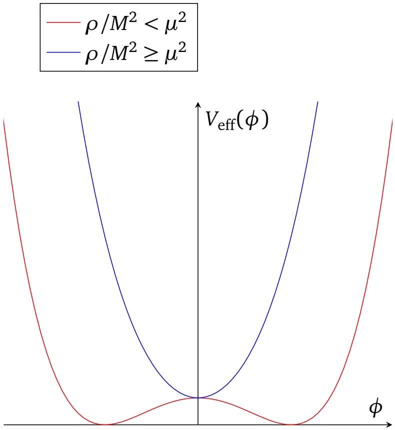

Figure 1: The symmetron effective potential.

The Symmetron Screening Mechanism

The Symmetron Screening Mechanism

A unit test mass experience a force given by $F = -\nabla \ln A(\phi) \approx -\frac{\phi}{M}\nabla\frac{\phi}{M}$

The Symmetron Screening Mechanism

A unit test mass experience a force given by $F = -\nabla \ln A(\phi) \approx -\frac{\phi}{M}\nabla\frac{\phi}{M}$

Low density $\Longrightarrow$ spontaneous symmetry breaking, nonzero vacuum expectation value v, unscreened force with coupling strength v/M.

The Symmetron Screening Mechanism

A unit test mass experience a force given by $F = -\nabla \ln A(\phi) \approx -\frac{\phi}{M}\nabla\frac{\phi}{M}$

Low density $\Longrightarrow$ spontaneous symmetry breaking, nonzero vacuum expectation value v, unscreened force with coupling strength v/M.

High density $\Longrightarrow$ symmetry is restored, $\phi \to 0$, fifth force is screened.

Constraints

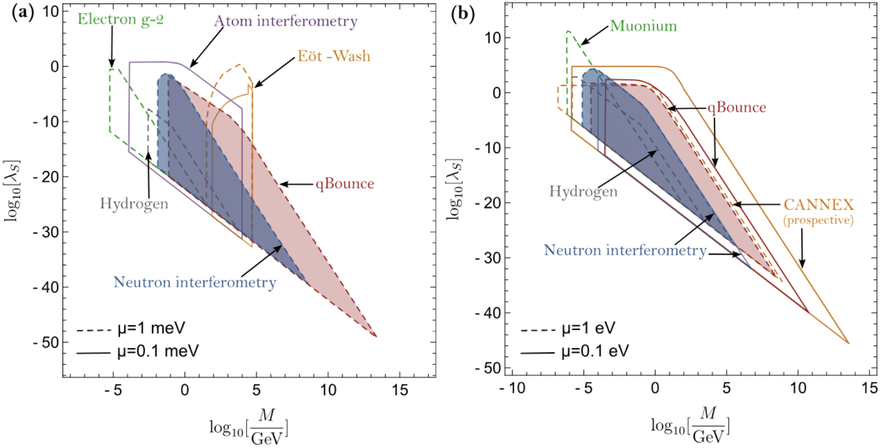

Figure 2: Constraints from H. Fischer, C. Käding and M. Pitschmann, 2024

Constraints

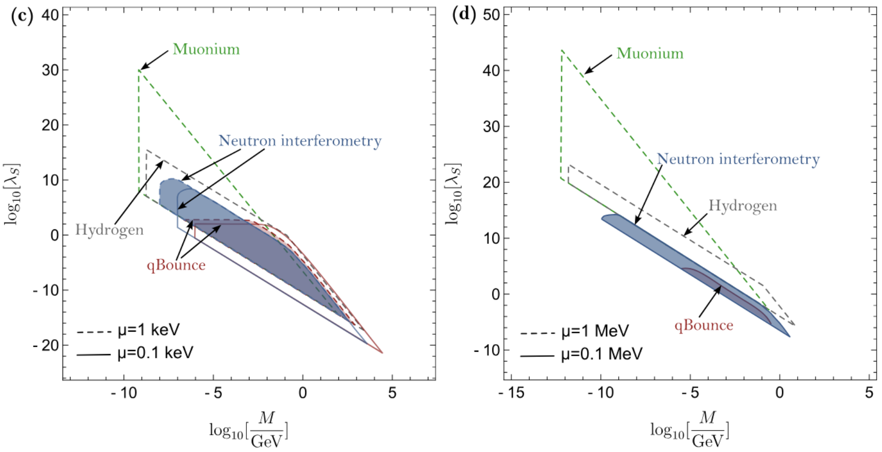

Figure 3: Constraints from H. Fischer, C. Käding and M. Pitschmann, 2024

Why Consider Quantum Corrections?

Why Consider Quantum Corrections?

Many predictions in the literature assume classical solutions.

Why Consider Quantum Corrections?

Many predictions in the literature assume classical solutions.

Field gradients become large in the vicinity of point-like sources (C. Burrage et al., 2021).

Why Consider Quantum Corrections?

Many predictions in the literature assume classical solutions.

Field gradients become large in the vicinity of point-like sources (C. Burrage et al., 2021).

One expects quantum corrections to be large when field gradients are (E. Weinberg, 2012).

Why Consider Quantum Corrections?

Many predictions in the literature assume classical solutions.

Field gradients become large in the vicinity of point-like sources (C. Burrage et al., 2021).

One expects quantum corrections to be large when field gradients are (E. Weinberg, 2012).

Field gradients are also large when the source is large compared to the field's Compton wavelength.

Why Consider Quantum Corrections?

Many predictions in the literature assume classical solutions.

Field gradients become large in the vicinity of point-like sources (C. Burrage et al., 2021).

One expects quantum corrections to be large when field gradients are (E. Weinberg, 2012).

Field gradients are also large when the source is large compared to the field's Compton wavelength.

Have we been missing significant quantum corrections to symmetron field profiles?

Method of External Sources

(B. Garbrecht and P. Millington, 2015)

Idea: Constrain the effective action by picking a *nonvanishing* external source.

Method of External Sources

(B. Garbrecht and P. Millington, 2015)
Idea: Constrain the effective action by picking a *nonvanishing* external source.
The effective action is defined by a Legendre transform,

$$\Gamma[\phi] = \max_J \left(W[J] - \int \mathrm{d}^4x\, J(x)\phi(x) \right) \equiv \max_J \Gamma_J[\phi]\,, \tag{2}$$

where J is a local source,

$$W[J] = -i \ln Z[J] \tag{3}$$

is the generating functional of connected correlation functions,

$$Z[J] = \int [\mathrm{d}\Phi] \exp\left[i \left(S[\Phi] + \int \mathrm{d}^4x\, J(x)\Phi(x) \right) \right] \tag{4}$$

is the generating functional of all correlation functions, and S is the classical action.

Method of External Sources

Source $\mathscr{J}$ which extremises Γ_J satisfies

$$\left.\frac{\delta\Gamma[\phi]}{\delta J(x)}\right|_{J=\mathscr{J}} = 0 \tag{5}$$

and defines

$$\Gamma[\phi] = W[\mathscr{J}] - \int \mathrm{d}^4x\, \mathscr{J}(x)\phi(x)\,. \tag{6}$$

The equation

$$\frac{\delta\Gamma[\phi]}{\delta\phi(x)} = -\mathscr{J}(x)[\phi] \tag{7}$$

yields the quantum field, provided a consistent choice for $\mathscr{J}$,

$$\mathscr{J}(x)[\phi] = 3i\lambda G(x)[\varphi_{\mathrm{cl}}]\varphi_{\mathrm{cl}}(x) \equiv \Pi(x)[\varphi_{\mathrm{cl}}]\varphi_{\mathrm{cl}}(x)\,. \tag{8}$$

Leading-Order Quantum Correction

Let $\phi_{\text{qu}}(x) = \phi_{\text{cl}}(x) + \delta\phi(x)$. Then

$$\delta\phi(x) = \int \mathrm{d}^4y\, G(x,y)\Pi^R(y)\phi_{\text{cl}}(y)\,, \tag{9}$$

where $G(x,y)$ is the propagator, defined by

$$\left.\frac{\delta^2 S[\phi]}{\delta\phi(x)\delta\phi(y)}\right|_{\phi=\phi_{\text{cl}}} G(x,y) = -\delta(x-y) \tag{10}$$

and $\Pi^R(x) = 3i\lambda G(x,x) + \delta m^2 + \delta\lambda\phi_{\text{cl}}(x)^2$ is the renormalised tadpole contribution.

Classical Solution

Static configuration,

$$\nabla^2\phi = \frac{\mathrm{d}V_{\mathrm{eff}}}{\mathrm{d}\phi} = \left(\frac{\rho(\mathbf{x})}{M^2} - \mu^2\right)\phi + \lambda\phi^3\,. \tag{11}$$

Classical Solution

Static configuration,

$$\nabla^2 \phi = \frac{\mathrm{d}V_{\text{eff}}}{\mathrm{d}\phi} = \left(\frac{\rho(\mathbf{x})}{M^2} - \mu^2 \right) \phi + \lambda \phi^3 \,. \tag{11}$$

Spherical source $\rho(\mathbf{x}) \to \rho(r) = \rho_0 \Theta(R - r)$,

$$\frac{\mathrm{d}^2 \phi}{\mathrm{d}r^2} + \frac{2}{r} \frac{\mathrm{d}\phi}{\mathrm{d}r} = \left(\frac{\rho(r)}{M^2} - \mu^2 \right) \phi + \lambda \phi^3 \,. \tag{12}$$

Classical Solution

Static configuration,

$$\nabla^2\phi = \frac{\mathrm{d}V_{\mathrm{eff}}}{\mathrm{d}\phi} = \left(\frac{\rho(\mathbf{x})}{M^2} - \mu^2\right)\phi + \lambda\phi^3 \,. \tag{11}$$

Spherical source $\rho(\mathbf{x}) \to \rho(r) = \rho_0\Theta(R-r)$,

$$\frac{\mathrm{d}^2\phi}{\mathrm{d}r^2} + \frac{2}{r}\frac{\mathrm{d}\phi}{\mathrm{d}r} = \left(\frac{\rho(r)}{M^2} - \mu^2\right)\phi + \lambda\phi^3 \,. \tag{12}$$

Thin-wall approximation: Assume $R \gg \mu^{-1}$. Then $2r^{-1}\mathrm{d}\phi/\mathrm{d}r \to 0$. Let $s = R - r$,

$$\frac{\mathrm{d}^2\phi}{\mathrm{d}s^2} = \left(\frac{\rho(s)}{M^2} - \mu^2\right)\phi + \lambda\phi^3 \,. \tag{13}$$

Classical Solution

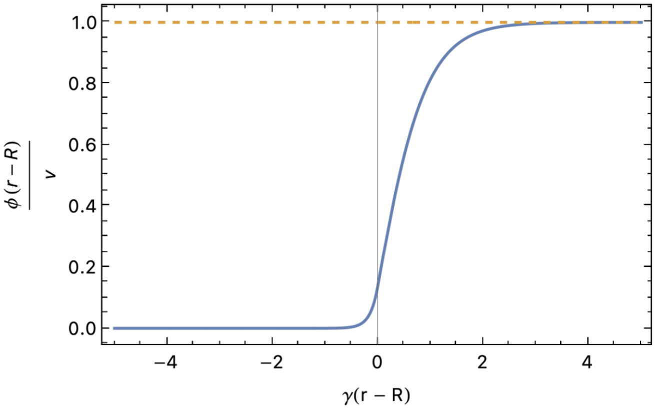

Figure 4: The classical symmetron field profile in the thin-wall approximation.

Green's Function

$G(x,x')$ determined by weighted sum over l and integral over E of $G_l(r,r';E)$, satisfying

$$\left(\frac{\mathrm{d}^2}{\mathrm{d}r^2} - \frac{l(l+1)}{r^2} + E^2 - \left. \frac{\mathrm{d}^2 V_{\mathrm{eff}}}{\mathrm{d}\phi^2} \right|_{\phi=\phi_{\mathrm{cl}}} \right) G_l(r,r';E) = \frac{\delta(r-r')}{r^2} \tag{14}$$

Green's Function

$G(x,x')$ determined by weighted sum over l and integral over E of $G_l(r,r';E)$, satisfying

$$\left(\frac{\mathrm{d}^2}{\mathrm{d}r^2} - \frac{l(l+1)}{r^2} + E^2 - \left. \frac{\mathrm{d}^2 V_{\mathrm{eff}}}{\mathrm{d}\phi^2} \right|_{\phi=\phi_{\mathrm{cl}}} \right) G_l(r,r';E) = \frac{\delta(r-r')}{r^2} \tag{14}$$

Thin-wall approximation

$$\left(\frac{\mathrm{d}^2}{\mathrm{d}s^2} - \frac{l(l+1)}{R^2} + E^2 - \left. \frac{\mathrm{d}^2 V_{\mathrm{eff}}}{\mathrm{d}\phi^2} \right|_{\phi=\phi_{\mathrm{cl}}} \right) G_l(s,s';E) = \frac{\delta(s-s')}{R^2} \tag{15}$$

Green's Function

$G(x,x')$ determined by weighted sum over l and integral over E of $G_l(r,r';E)$, satisfying

$$\left(\frac{\mathrm{d}^2}{\mathrm{d}r^2} - \frac{l(l+1)}{r^2} + E^2 - \left.\frac{\mathrm{d}^2 V_{\mathrm{eff}}}{\mathrm{d}\phi^2}\right|_{\phi=\phi_{\mathrm{cl}}}\right) G_l(r,r';E) = \frac{\delta(r-r')}{r^2} \tag{14}$$

Thin-wall approximation

$$\left(\frac{\mathrm{d}^2}{\mathrm{d}s^2} - \frac{l(l+1)}{R^2} + E^2 - \left.\frac{\mathrm{d}^2 V_{\mathrm{eff}}}{\mathrm{d}\phi^2}\right|_{\phi=\phi_{\mathrm{cl}}}\right) G_l(s,s';E) = \frac{\delta(s-s')}{R^2} \tag{15}$$

Planar limit

$$\frac{l(l+1)}{R^2} \approx p^2 \Longrightarrow \sum_l (2l+1) \to \int \mathrm{d}p\, p \tag{16}$$

Potential

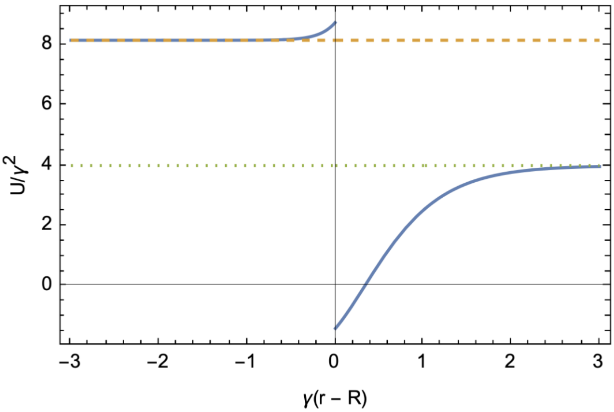

Figure 5: The potential for the Green's function and eigenfunction problem.

Decomposition

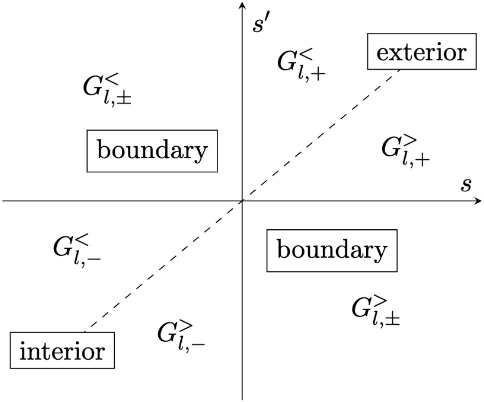

Figure 6: A graphical depiction of the decomposition of the Green's function in the s, s'-plane.

Coincident Green's Function

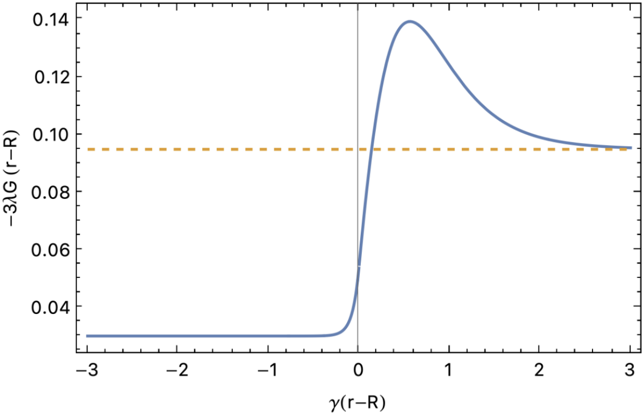

Figure 7: The coincident Green's function in position space.

Tangent: What if we don't take the thin wall approximation?

The 1D equation of motion also describes very long rods or very large planes.

Tangent: What if we don't take the thin wall approximation?

The 1D equation of motion also describes very long rods or very large planes. In this way, the system of equations

$$\frac{\mathrm{d}^2\phi}{\mathrm{d}x^2} = \left(\frac{\rho_0 \operatorname{rect}\left(\frac{x}{2R}\right)}{M^2} - \mu^2\right)\phi + \lambda\phi^3\,;\ \phi'(0) = 0, \phi(\pm\infty) = v \tag{17}$$

captures cylindrical-planar symmetry, as opposed to the spherical-planar symmetry of the thin-wall approximation.

1D is Harder Than 3D (plus approximations)

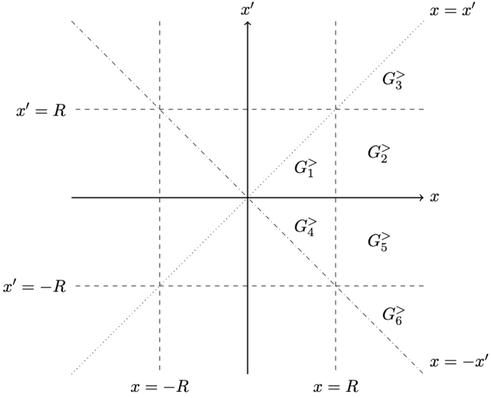

Figure 8: A graphical depiction of the decomposition of the Green's function in the x, x'-plane.

Renormalisation

Renormalisation conditions

$$\left.\frac{\mathrm{d}^2 V_{\text{1-loop}}}{\mathrm{d}\phi^2}\right|_{\phi=v} = 2\mu^2 \text{ and } \left.\frac{\mathrm{d}^4 V_{\text{1-loop}}}{\mathrm{d}\phi^4}\right|_{\phi=v} = 6\lambda \tag{18}$$

determine counterterms δm^2 and $\delta\lambda$.

Renormalisation

Renormalisation conditions

$$\left.\frac{\mathrm{d}^2 V_{\text{1-loop}}}{\mathrm{d}\phi^2}\right|_{\phi=v} = 2\mu^2 \text{ and } \left.\frac{\mathrm{d}^4 V_{\text{1-loop}}}{\mathrm{d}\phi^4}\right|_{\phi=v} = 6\lambda \tag{18}$$

determine counterterms δm^2 and $\delta\lambda$.Counterterms determine *pseudocounterterms*,

$$\frac{1}{2\pi^2}\int_0^\Lambda \mathrm{d}p\, p^2 \Delta m^2(p) = \delta m^2 \text{ and } \frac{1}{2\pi^2}\int_0^\Lambda \mathrm{d}p\, p^2 \Delta\lambda(p) = \delta\lambda\,. \tag{19}$$

Renormalisation

Renormalisation conditions

$$\left.\frac{\mathrm{d}^2 V_{\text{1-loop}}}{\mathrm{d}\phi^2}\right|_{\phi=v} = 2\mu^2 \text{ and } \left.\frac{\mathrm{d}^4 V_{\text{1-loop}}}{\mathrm{d}\phi^4}\right|_{\phi=v} = 6\lambda \tag{18}$$

determine counterterms δm^2 and $\delta\lambda$.Counterterms determine *pseudocounterterms*,

$$\frac{1}{2\pi^2}\int_0^\Lambda \mathrm{d}p\, p^2 \Delta m^2(p) = \delta m^2 \text{ and } \frac{1}{2\pi^2}\int_0^\Lambda \mathrm{d}p\, p^2 \Delta\lambda(p) = \delta\lambda\,. \tag{19}$$

Pseudocounterterms facilitate numerical computation of the tadpole contribution,

$$\Pi^R(x) = \frac{1}{2\pi^2}\int_0^\Lambda \mathrm{d}p\, p^2 \left(-3\lambda G(s,s) + \Delta m^2 + \Delta\lambda\phi^2\right)\,. \tag{20}$$

Quantum-Corrected Field

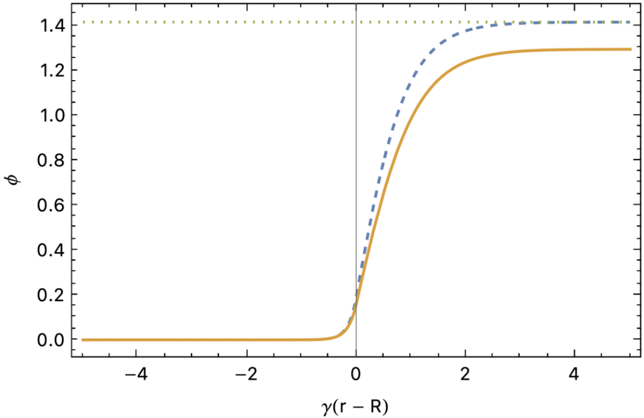

Figure 9: The classical (blue, dashed) and quantum (orange, solid) symmetron field profiles.

Some Analytical Understanding

Shift in the vev Δv,

$$\left.\frac{\partial V_{\text{1-loop}}}{\partial \phi}\right|_{v+\Delta v} = 0 \Rightarrow \Delta v = -\frac{27\lambda}{16\pi^2} v + O(\lambda^2)\,, \tag{21}$$

changes the asymptotic value.

Some Analytical Understanding

Shift in the vev Δv,

$$\left.\frac{\partial V_{\text{1-loop}}}{\partial \phi}\right|_{v+\Delta v} = 0 \Rightarrow \Delta v = -\frac{27\lambda}{16\pi^2} v + O(\lambda^2)\,, \tag{21}$$

changes the asymptotic value.

Shift in the mass,

$$m_{\text{1-loop}} = \left.\frac{\partial^2 V_{\text{1-loop}}}{\partial \phi^2}\right|_{v+\Delta v} = 2\mu^2\left(1 - \frac{81\lambda}{16\pi^2}\right) + O(\lambda^2)\,, \tag{22}$$

changes the slope.

Slope Shift

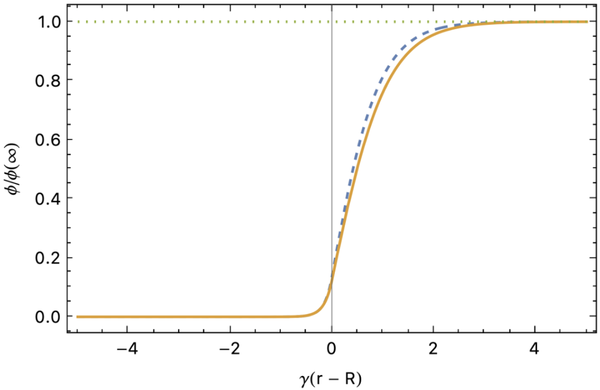

Figure 10: The classical (blue, dashed) and quantum (orange, solid) symmetron field profiles, normalised to their asymptotic values.

Quantum-Corrected Force

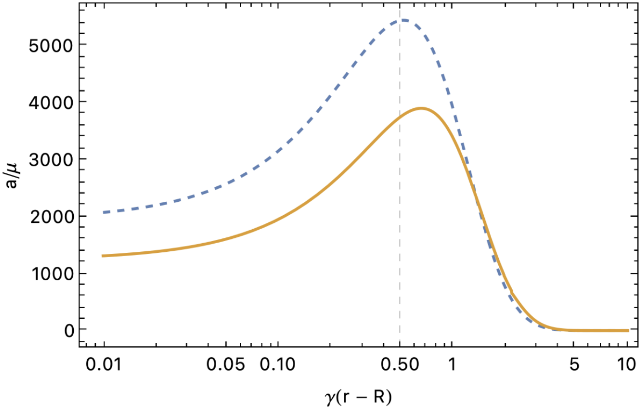

Figure 11: The classical (blue, dashed) and quantum (orange, solid) symmetron fifth force profiles. $\mu = 1\text{GeV}$, $M = 10\text{MeV}$, $\lambda = 0.5$, $\rho_0 = 2.45 \times 10^{-3}\text{GeV}^4$ (hydrogen spectroscopy)

Quantum-Corrected Force

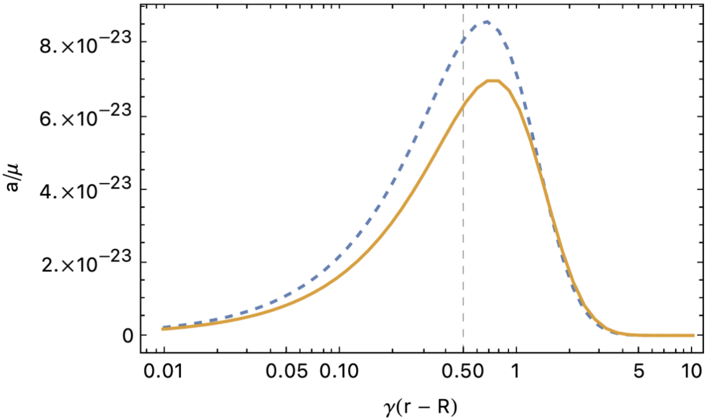

Figure 12: The classical (blue, dashed) and quantum (orange, solid) symmetron fifth force profiles. $\mu = 10^{-1}$meV, $M = 10^{-2}$GeV, $\lambda = 10^{-0.5}$, $\rho_0 = 8.178 \times 10^{-5}$MeV^4 (atom interferometry)

Some More Analytical Understanding

In the vicinity of a source which produces a symmetron field profile ϕ, a test particle experiences an acceleration

$$a = -\frac{1}{M^2}\phi\nabla\phi \; . \tag{23}$$

Some More Analytical Understanding

In the vicinity of a source which produces a symmetron field profile ϕ, a test particle experiences an acceleration

$$a = -\frac{1}{M^2}\phi\nabla\phi \ . \tag{23}$$

Very roughly, one might expect the vev shift to contribute twice and the mass shift once to the quantum correction in a,

$$\Delta F = \frac{a_{\rm cl} - a_{\rm qu}}{a_{\rm cl}} \sim 2 \times \frac{27\lambda}{16\pi^2} + \frac{81\lambda}{32\pi^2} \approx \frac{6\lambda}{\pi^2} \ . \tag{24}$$

Some More Analytical Understanding

In the vicinity of a source which produces a symmetron field profile ϕ, a test particle experiences an acceleration

$$a = -\frac{1}{M^2}\phi\nabla\phi \ . \tag{23}$$

Very roughly, one might expect the vev shift to contribute twice and the mass shift once to the quantum correction in a,

$$\Delta F = \frac{a_{\mathrm{cl}} - a_{\mathrm{qu}}}{a_{\mathrm{cl}}} \sim 2 \times \frac{27\lambda}{16\pi^2} + \frac{81\lambda}{32\pi^2} \approx \frac{6\lambda}{\pi^2} \ . \tag{24}$$

In other words, we should expect virtually no μ-dependence and approximately linear λ-dependence in ΔF.

μ-dependence

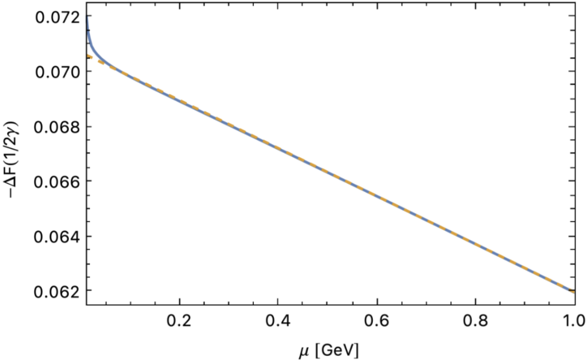

Figure 13: The dependence of the relative shift in the force on the mass μ, at one Compton wavelength from the surface of the source.

λ-dependence

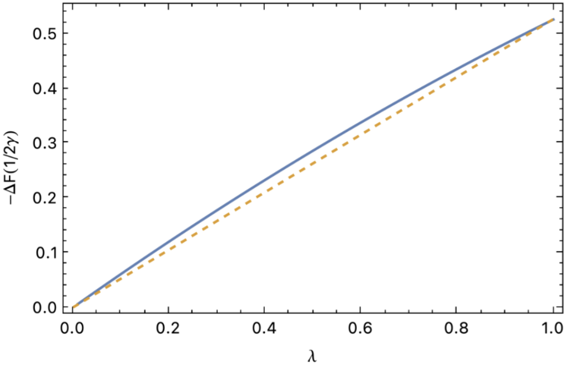

Figure 14: The dependence of the relative shift in the force on the self-coupling λ, at one Compton wavelength from the surface of the source.

Conclusions

Our results provide a first estimate of the theoretical uncertainty on existing fifth force predictions that neglect radiative effects.

Conclusions

Our results provide a first estimate of the theoretical uncertainty on existing fifth force predictions that neglect radiative effects.

For large spherical and planar geometries, the quantum corrections to the symmetron field profile can weaken the fifth force by as much as 50% *locally*.

Conclusions

Our results provide a first estimate of the theoretical uncertainty on existing fifth force predictions that neglect radiative effects.

For large spherical and planar geometries, the quantum corrections to the symmetron field profile can weaken the fifth force by as much as 50% *locally*.

The quantum correction to the field varies spatially. It cannot be fine-tuned away.

Conclusions

Our results provide a first estimate of the theoretical uncertainty on existing fifth force predictions that neglect radiative effects.

For large spherical and planar geometries, the quantum corrections to the symmetron field profile can weaken the fifth force by as much as 50% *locally*.

The quantum correction to the field varies spatially. It cannot be fine-tuned away.

Higher-order corrections are likely also relevant.

Conclusions

Our results provide a first estimate of the theoretical uncertainty on existing fifth force predictions that neglect radiative effects.

For large spherical and planar geometries, the quantum corrections to the symmetron field profile can weaken the fifth force by as much as 50% *locally*.

The quantum correction to the field varies spatially. It cannot be fine-tuned away.

Higher-order corrections are likely also relevant.

The magnitude of the correction to the force scales almost linearly with the self-coupling.

Conclusions

Our results provide a first estimate of the theoretical uncertainty on existing fifth force predictions that neglect radiative effects.

For large spherical and planar geometries, the quantum corrections to the symmetron field profile can weaken the fifth force by as much as 50% *locally*.

The quantum correction to the field varies spatially. It cannot be fine-tuned away.

Higher-order corrections are likely also relevant.

The magnitude of the correction to the force scales almost linearly with the self-coupling.

Current constraints may be weaker than we thought, especially for nonperturbative self-couplings.